ISSN/2499-5347

R. CARCIONE, I. DI SARCINA, G. FERRARA, J. SCIFO, A. VERNA, AND A. CEMMI

Fusion and Technology for Nuclear Safety and Security Department
Innovative Nuclear Systems Laboratory
Casaccia Research Centre, Rome - Italy

B. D'ORSI

Sapienza University, Roma

OPTIMIZATION OF PAPER CHARACTERIZATION PROCEDURES FOR CULTURAL HERITAGE

RT/2024/2/ENEA

ITALIAN NATIONAL AGENCY FOR NEW TECHNOLOGIES,
ENERGY AND SUSTAINABLE ECONOMIC DEVELOPMENT

R. CARCIONE, I. DI SARCINA, G. FERRARA,
J. SCIFO, A. VERNA, AND A. CEMMI

Fusion and Technology for Nuclear Safety
and Security Department
Innovative Nuclear Systems Laboratory
Casaccia Research Centre, Rome - Italy

B. D'ORSI

Sapienza University, Roma

OPTIMIZATION OF PAPER CHARACTERIZATION PROCEDURES FOR CULTURAL HERITAGE

RT/2024/2/ENEA

ITALIAN NATIONAL AGENCY FOR NEW TECHNOLOGIES,
ENERGY AND SUSTAINABLE ECONOMIC DEVELOPMENT

OPTIMIZATION OF PAPER CHARACTERIZATION PROCEDURES FOR CULTURAL HERITAGE

B. D'Orsi, R. Carcione, I. Di Sarcina, G. Ferrara, J. Scifo, A. Verna and A. Cemmi

Abstract

Conservation and preservation of Cultural Heritage is of paramount importance to maintain the national identity. Ionizing radiation treatments are worldwide applied for conservation of artworks made from materials of organic origin (paper, wood, parchment, etc.) but in Italy they are not fully accepted probably due to the incorrect knowledge of the radiation induced effects on the artifacts. In this regard, the investigation of these secondary effects and of their minimization plays a key role. In this report, established procedures for the physico-chemical characterization of paper, before.

Key words: *gamma irradiation, paper, Cultural Heritage conservation, characterization techniques.*

OTTIMIZZAZIONE DELLE PROCEDURE DI CARATTERIZZAZIONE DELLA CARTA PER APPLICAZIONI NEL CAMPO DEI BENI CULTURALI

Riassunto

La conservazione dei Beni Culturali è di importanza fondamentale per sostenere l'identità nazionale. Trattamenti con le radiazioni ionizzanti vengono utilizzati in tutto il mondo per la conservazione di opere d'arte costituite da materiali di origine naturale (carta, legno, pergamena) ma in Italia non sono ancora accettati del tutto, probabilmente a causa della non corretta conoscenza degli effetti indotti dalla radiazione sul manufatto. Da questo punto di vista, lo studio approfondito di questi effetti secondari e delle condizioni di irraggiamento che permettono di minimizzarli riveste un ruolo centrale. In questo report sono descritte procedure convalidate di caratterizzazione fisico chimica della carta, prima e dopo irraggiamento, con diverse tecniche sperimentali.

Parole chiave: irraggiamento gamma, carta, Beni Culturali, trattamenti di conservazione, tecniche di caratterizzazione.

INDEX

Introduction

The conservation of Cultural Heritage (CH) is of great importance considering the Italian artistic, cultural and historic heritage. Radiation processing can be applied to perform preservation treatments in CH and they are widely used in several countries since they represent a powerful technique for the disinfection and disinfestation of natural origin artifacts (such as paper, wood, textiles, parchment).

Gamma radiation treatments show several and indisputable advantages over classical conservation procedures because of the high penetration power of this kind of radiation that allows to treat large and multi-material objects of different sizes in a short time. Nevertheless, ionizing radiation conservation processing is still not fully accepted by the italian CH community, due to the often incorrect knowledge of the physico-chemical modifications (secondary effects) induced by radiation on the treated materials [1]. For this reason, it is crucial to provide reliable and specific results, obtained by different techniques widely accepted and recognized, describing the secondary effects occurrence.

Paper is one of the most common and fragile CH materials and it is characterized by high variability in terms of composition and conservation state. Moreover, since the possible changes induced by gamma radiation applied for conservation treatment (low absorbed dose range, < 10 kGy) are often slightly detectable, it is really important to follow specific and reliable data analysis procedures to avoid misinterpretation of the experimental results. For these reasons, the aim of this technical report is to define the optimization of the procedures used for paper characterization in CH field.

Microscopic and macroscopic changes caused by gamma radiation on paper can be evaluated by characterization techniques performed before and after irradiation. In particular, gamma radiation can induce the formation of new chemical bonds (crosslinking) or the breaking of the polymeric network (depolymerization) of cellulose, depending on the absorbed dose [2]. Besides, a huge number of free radicals, responsible of long-lasting post-irradiation changes, are produced into the cellulose network.

Finally, a key role is played by the oxygen present in the air and by the environmental humidity. During the irradiation, oxygen can diffuse in the bulk of the objects, causing the formation of oxygen-containing very energetic radicals which are able to react with the surrounding molecules, inducing oxidation and degradation in the thickness of material permeated by oxygen (oxidative degradation) [3]–[5]. The oxidation of cellulose is mainly related to the formation of carbonyl groups (C= O) responsible of different effects, such as

color changes (yellowing or even browning) and/or network modifications. Whether oxidation increases, a reduction of the polymerization degree (DP) or eventually mechanical properties modification and consequent paper embrittlement could be observed [6]–[8] with the dose increase.

The investigation of the above-described gamma radiation-induced effects on cellulose-based materials can be carried out by using several experimental techniques.

In this report, an optimization of the characterization procedures of paper by means of Fourier Transform Infrared (FTIR) spectroscopy, Electron Spin Resonance (ESR) spectroscopy, viscosity measurements and colorimetric measurements is described. The choice of experimental techniques for the characterization of the samples before and after irradiation has tried to privilege the availability and ease-to-use of methods not invasive and not destructive as much as possible. The experimental activities described in the present report were performed at the Calliope gamma irradiation facility (ENEA Casaccia R.C., Rome, Italy).

1 Materials

This report is focused on the optimization of the characterization procedures of paper since cellulose-containing substrates, such as paper and wood, are very commonly used in several CH artworks (ancient books, documents, archived materials, wooden statues, etc.). In particular, these procedures have been applied to Whatman paper, used as new reference material since it is composed of high quality cotton fibers and has a cellulose content >98%, and to an ancient book.

1.1 Reference paper

Whatman paper No. 1 (thickness = 0.20 mm, Carlo Erba, Italy) [9], consists of pure cellulose, a polysaccharide composed of a linear polymer, based on β-D-glucose monomers linked together by means of β-1,4-glycosidic bond, giving long chains and partially ordered structures [2], [10]. The cellulose network is characterized by the presence of intra- and inter-molecular hydrogen bonds systems (Fig. 1).

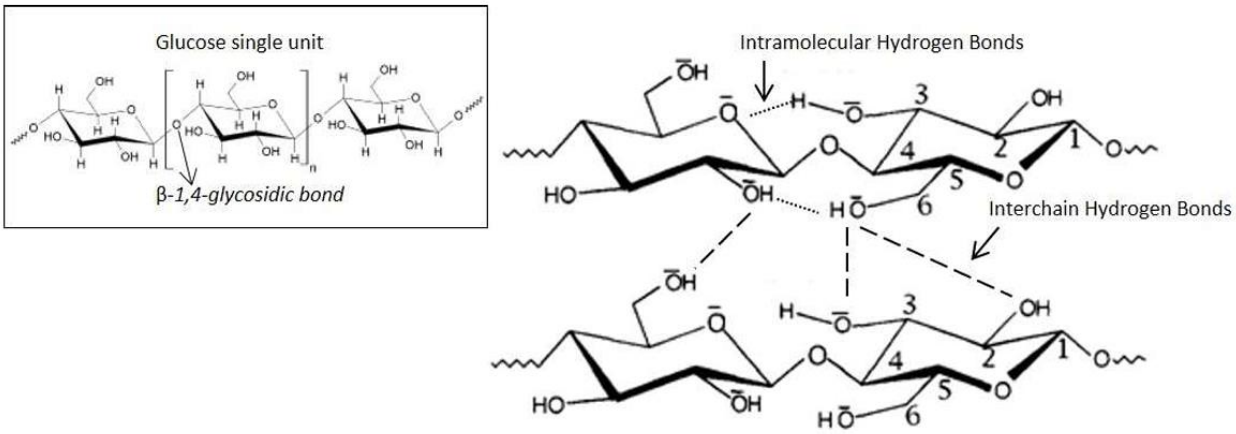

Figure 1 - Cellulose network with intra- (dashed lines) and inter- molecular hydrogen bonds (wrinkle lines). Inset: structure of a cellulose chain.

1.2 Ancient paper

Papery and archived CH are characterized by an extremely wide variability in term of composition. It is possible to find papers that contain additives such as lignin, sugar, calcium carbonate, glues, whiteners that present different properties with respect to Whatman. In particular, lignin units are easily identifiable by spectroscopic techniques since they contain double C=C bonds. Furthermore, old books can be damaged by bad storage conditions and may present microbial growth which can cause a deterioration of the paper physico-chemical properties such as DP drop or color inhomogeneity. Therefore, especially for some kind of analysis the optimization of the measurement procedure of ancient paper is needed. In Figure 2, the photos of the back cover (Fig 2a) and of the central pages (Fig. 2b) of an old book (1890) analyzed for this report are shown.

Figure 2 – Back cover (a) and central pages (b) of an old book (1890).

2 Methods

The paper samples are characterized by means of different experimental techniques (as described in the following paragraphs) before and after gamma irradiation to evaluate the changes induced by the radiation treatment.

2.1 Calliope gamma irradiation facility

The Calliope gamma irradiation facility is a pool-type facility equipped with a ^{60}Co radio-isotopic source array in a large volume (7.0x6.0x3.9 m) shielded cell [11]. The source rack is composed of 25 ^{60}Co source rods (with an active area of 41x90 cm) placed in a planar geometry (Fig. 3).

Figure 3 - a) Calliope source rack in the pool and b) source rack within the irradiation cell (picture acquired by remote camera).

The maximum licensed activity for the Calliope plant is $3.7 \cdot 10^{15}$ Bq (100 kCi) and, positioning a sample at different distances with respect to the source rack, within the irradiation cell, it is possible to perform irradiation at different dose rate values; in particular, the maximum available dose rate is currently 6.2 kGy/h (December 2023). The steel platform, shown in Fig. 3b, is installed to perform irradiation at high dose rate values. It is also possible to perform irradiation tests in different environmental conditions. A dosimetric laboratory and a characterization laboratory are also available at the Calliope facility.

2.2 Characterization techniques

The paper characterization procedure described in this technical report is performed by the following experimental techniques.

2.2.1 Micro-Raman imaging

Raman spectroscopy provides information about the molecular structure of samples. A micro-Raman spectrometer combines Raman spectroscopy with optical microscopy, allowing for the analysis of localized areas of a sample. A XploRA Plus micro-Raman spectrometer (Fig. 4) by HORIBA was employed to obtain optical microscope images and Raman spectra of samples.

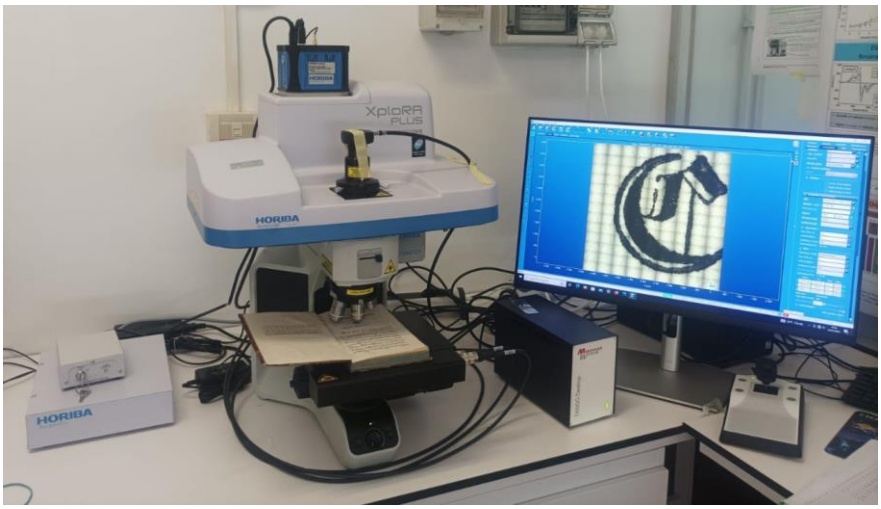

Figure 4 - HORIBA XploRA PLUS Raman instrument.

The Raman spectroscope uses a 785 nm laser that enables to perform Raman spectra in the range 100 – 3200 cm^{-1}. The instrument is endowed with a true confocal microscope that allows transmission or reflection illumination to perform high quality 2D and 3D imaging with 5x, 10x and 100x objectives.

The HORIBA XploRA PLUS Raman instrument sample holder allows the analysis of materials with dimensions scalable from few microns up to macroscopic objects. Being a non-destructive technique, the micro-Raman analysis can be carried out directly on book samples.

2.2.2 FTIR/FTIR-ATR spectroscopy

FTIR spectroscopy is useful to investigate the chemical composition and the oxidation states variation of samples. This technique uses the interaction between infrared light and matter and allows to obtain the frequencies of light that are absorbed by the sample to identify and quantify different chemical species [12]. Spectrum 100 FT-IR spectrometer by Perkin-Elmer was used for this study. This spectrometer allows measurements in the range 400-7000 cm^{-1} and in the dark, in air or in inert gas atmosphere and can be equipped with a gold integrating

sphere. The FTIR spectrometer can be used in transmission and attenuated total reflectance (ATR) configuration as shown in Figure 5.

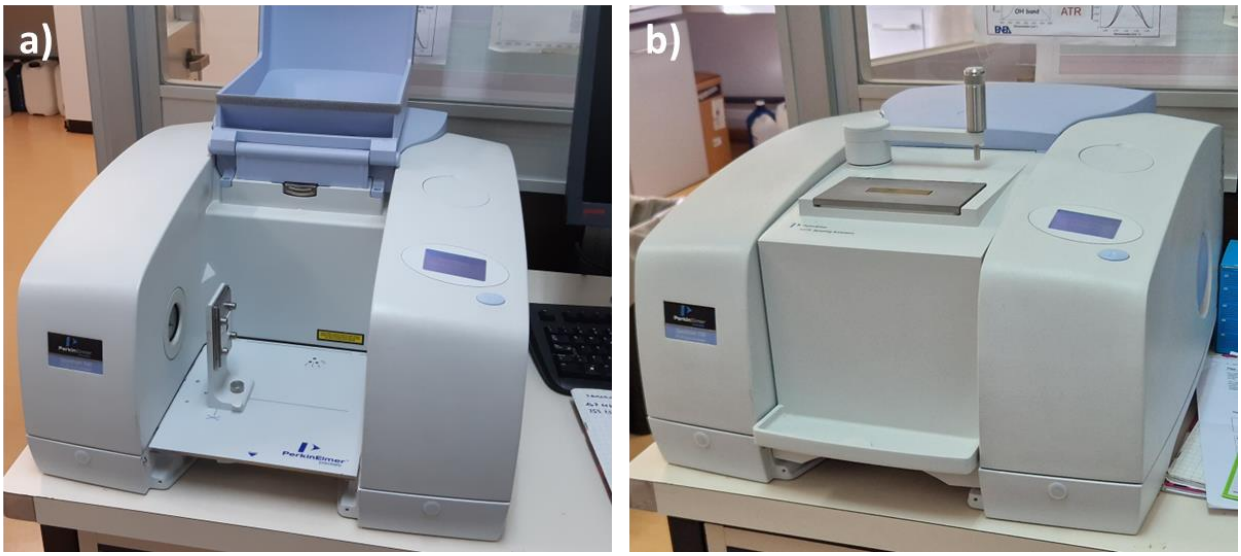

Figure 5 - Spectrum 100 FT-IR spectrometer by Perkin-Elmer with a) transmission and b) ATR accessory.

2.2.3 ESR spectrometry

ESR spectroscopy is useful to investigate the behavior of free radical species. The ESR spectra are the first derivative of the physical signal (absorption of photons which allows the transition of the unpaired electron of a molecule from an energy state to another [13]). The ESR signal is proportional to the free radicals number presents in the samples. In this study, ESR spectra were obtained by using an ESR Bruker *e*-scan spectrometer (Fig. 6) operating in the X-band with a frequency of 9.4 GHz, microwave power of 0.14 mW and magnetic field in the range 3390–3580 G.

Figure 6 - ESR Bruker *e*-scan spectrometer.

2.2.4 Rheometric analysis

A rheometer is used to measure viscosimetric properties of liquid or fluid samples. For paper samples, the procedure described in the ISO:5351:2012 standard regulation can be followed [14]. In this work, viscosimetric analysis was used to obtain polymerization degree (DP) values which are related to mechanical properties of paper samples, that are very important in CH conservation. Viscosity measurements were carried out with a TA Instrument AR 2000 rheometer (Fig. 7a), at room temperature, equipped with two parallel plates (Fig. 7b).

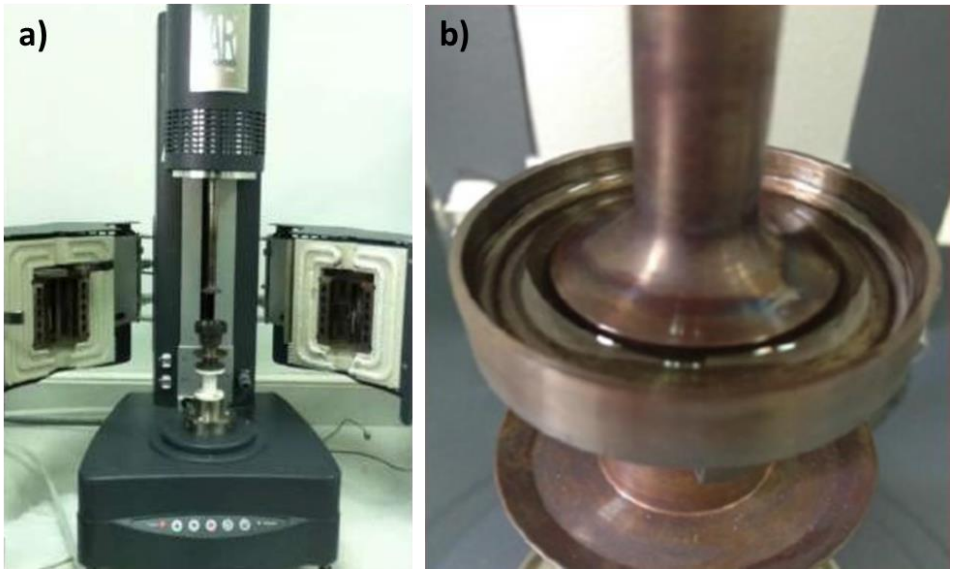

Figure 7 - TA Instrument AR 2000 rheometer (a) equipped with two parallel plates (b).

The first fixed plate, where the sample is placed in solution [14], is mounted at the base of the instrument and the second rotating one is connected to the top of the rheometer. The viscosity η of a material is defined as its resistance to deform when it is subjected to a stress and it is given by the ratio:

$$\eta = \frac{\tau}{\dot{\gamma}} \; [Pa \cdot s] \tag{1}$$

where τ is the shear stress and $\dot{\gamma}$ is the shear rate [15].

2.2.5 Colorimetry

Colorimetric measurements enable to quantify and describe the human perception of colors by replacing subjective responses with an objective numerical system. In this study, the colorimetric analysis was performed by a PCE-CSM 8 colorimeter by PCE Instruments (Fig. 8) endowed with a 3.5″ touch screen display.

Figure 8 – PCE-CSM 8 colorimeter.

The colors evaluation method is based on the use of the CIE 1931 System of Colorimetry, defined by the International Commission on Illumination (Commission Internationale d'Eclairage: CIE) in 1931 [16]. Each visible color has a non-negative coordinates in the 3D XYZ color space. The colorimeter allows to show the color in different color spaces. In this report, the CIE 1931 xyY and the CIELAB color space are used. The CIELAB color space allows to identify the color by the chromaticity coordinates L*, a* and b* [17], [18]. Furthermore, it is possible to define the parameter ΔE* which gives information about color differences (defined as Euclidian distances in CIELAB [19]) among the analyzed samples to evaluate color changes due to irradiation. In particular, if $\Delta E^* < 3$ the color difference is not visually appreciable, if $3 < \Delta E^* < 6$ the difference is appreciable but acceptable while if $\Delta E^* > 6$ it is not acceptable [20].

3 Optimization of procedures

The samples preparation and the optimized measurements procedures are described in the following.

3.1 Paper samples

A new Whatman paper sheet and central pages of the old book were cut to obtain the samples used for the characterization with the above-described experimental techniques. The main goal of the reported characterization is to evaluate the gamma radiation-induced changes in the samples and to find the irradiation parameters that minimize these changes. Therefore, the first step consists of defining the irradiation conditions (dose and dose rate) to be used for the treatment. Then, a set of samples for each established irradiation condition is prepared. In this way, each set of samples is irradiated at certain conditions and its features can hence be analyzed over time (useful e.g. for ESR analysis). An additional samples set is prepared but not irradiated and used as reference. Each set is composed of one paper sample of about 20 mm x 30 mm for Micro-Raman, FTIR and colorimetric measurements, one strip of about 15 mm for ESR measurements and one 12 mg sample for viscosity measurements.

The irradiation and the characterization measurements were performed at the Calliope gamma irradiation facility and laboratory, keeping the samples in air and at room temperature.

3.2 Micro-Raman analysis

For the Raman analysis protocol, the procedure for the acquisition of the images by the microscope and of the spectra were optimized.

Pictures of samples were acquired with a 10x objective microscope. The Raman spectra were recorded with 10x and 100x objective magnifications in the spectral range 200 - 3000 cm^{-1} with a 785 nm laser excitation, 50mW laser power and a diffraction grating of 1200 gr/mm. Before the analysis, Raman spectra were background subtracted and smoothed.

The HORIBA's XploRA PLUS confocal microscope can operate in both transmission and reflection modes. To adapt the protocol to remarkably thick paper samples, the images were acquired by using only reflected illumination. Figure 9 shows the optical microscope images collected on a reference Whatman paper sample with a 5x, 10x and 100x objective. The illumination was set at 100% for the images taken at 5x, while the pictures at 10x and 100x were acquired at the illumination at 70%.

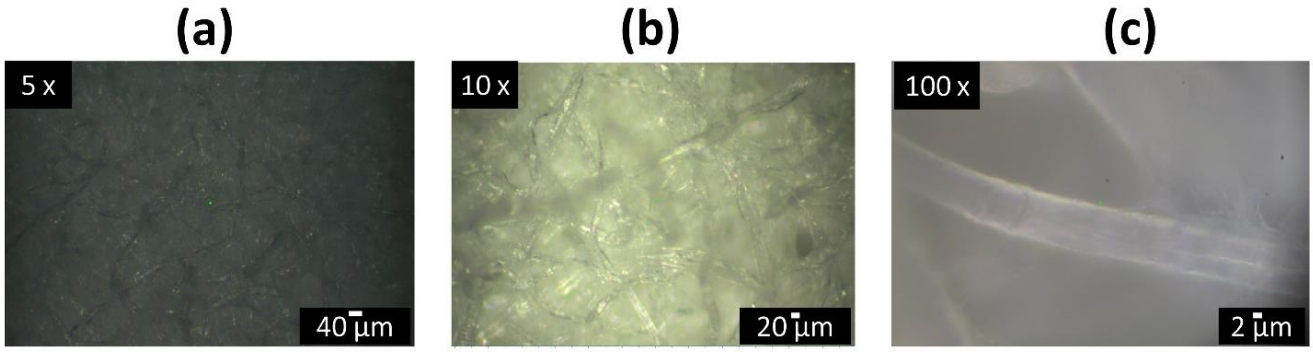

Figure 9 - Whatman paper optical images acquired with (a) 5 (b) 10 and (c) 100x objective.

As shown in Figure 9a, the dark images taken at 5x objective and the reflected illumination at 100% do not allow to clearly visualize the paper's texture. On the contrary, the pictures recorded at 10x (Fig. 9b) by setting the illumination at 70% disclose the cellulose fibrillar entities on the paper surface. The images at 100x (Fig. 9c) do not give information on the texture of the paper, however, are useful to obtain details of the fibrillar structures.

On these bases, the microscope image acquisition was optimized by setting the objective at 10x. In Figure 10, the optical microscope images acquired on a reference Whatman paper sample with the illumination at 40%, 50%, 60%, 70%, 80% and 90%, are shown.

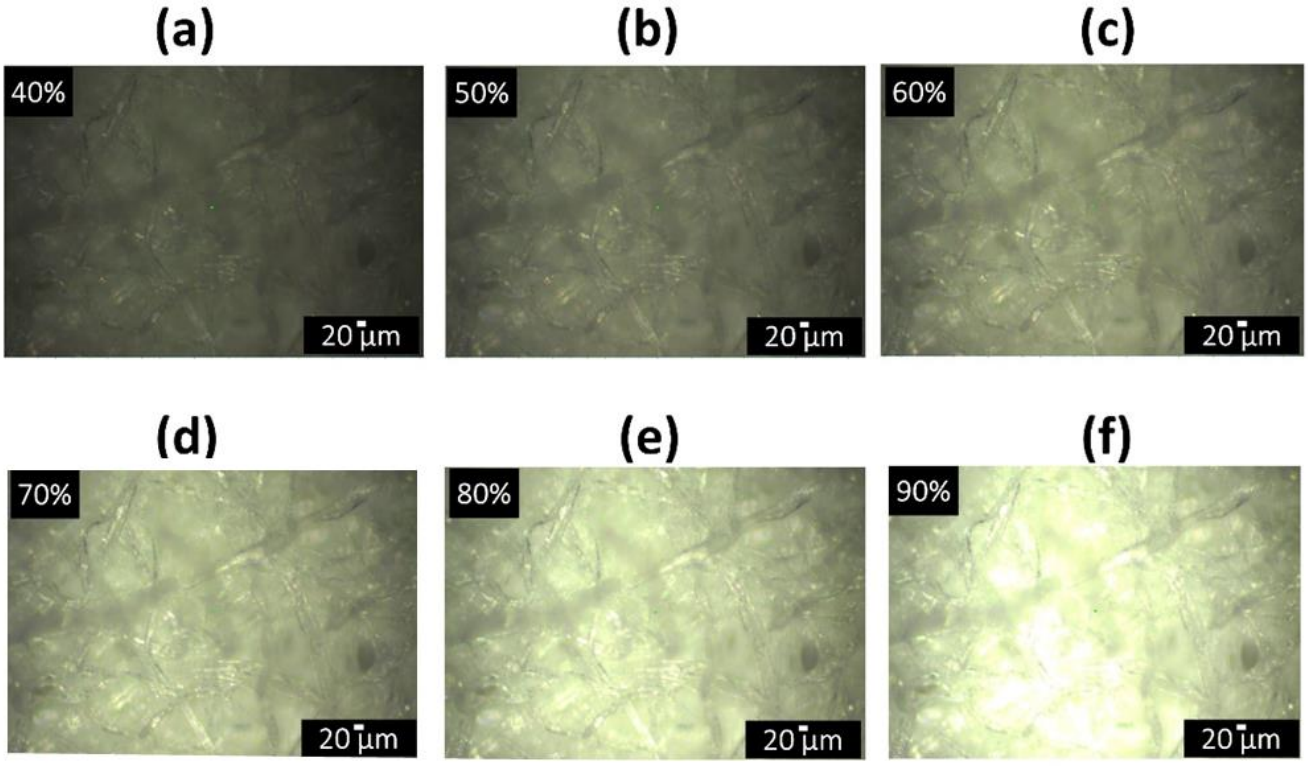

Figure 10 - Optical microscope images acquired on a reference Whatman paper sample with the illumination at (a) 40%, (b) 50%, (c) 60%, (d) 70%, (e) 80% and (f) 90%.

From Figure 10, it is evident that illumination is a crucial parameter for images acquisition quality: in particular, an illumination lower than 70% produces rather dark images. Conversely, illumination at 80% and 90% is significantly bright, determining the losing of details. Given such considerations, the optimized conditions to acquire the best optical microscope images are 10x objective with a reflected illumination of 70%.

To optimize the parameters for the spectral acquisition, Raman signals were recorded in the range 200 – 3000 cm^{-1} at different objective magnification. In Figure 11, the Raman spectra acquired on reference Whatman paper samples at the magnification of 10x and 100x are shown.

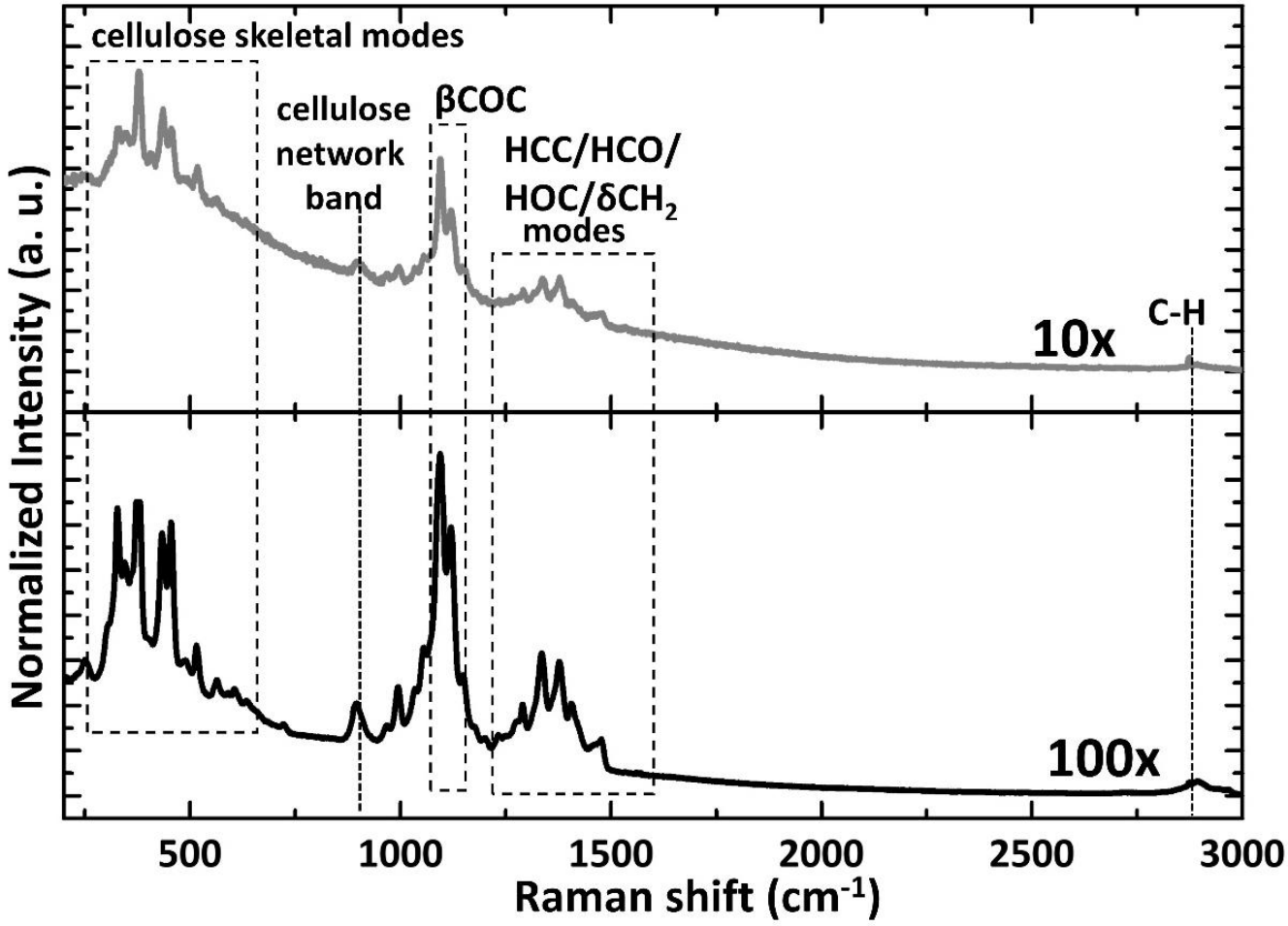

Figure 11 - Raman spectra acquired on reference Whatman paper samples at the magnification of 10x and 100x.

As shown in Figure 11, with both the magnification values, the Raman spectra exhibit the typical signals ascribable to cellulose. In the range 200 - 700 cm^{-1} the peaks assignable to the cellulose skeletal modes [21] are located, while the range 800 - 1700 cm^{-1} contains the signals ascribed to the cellulose network band, the β-glycosidic βCOC vibrations and the HCC/HCO/HOC/δCH2 modes [22]–[31]. Furthermore, the bands corresponding to the CH stretching vibrations are located around 2900 cm^{-1}.

Although the cellulose signals are distinguishable in both spectra shown in Figure 11, it must be considered that the Raman spectral acquisition with 10x objective produces a worse signal/noise ratio reasonably due to light scattering phenomena. In contrast, acquisition with 100x objective produces a rather smooth spectrum where the cellulose signals in the range 800 - 1700 cm^{-1} are sharp and well-defined.

Furthermore, Raman spectra acquired with 100x objective allow to investigate ancient and new paper samples, independently on the content of additives such as lignin. Considering that the lignin phase in paper produces Raman signals around 1600 cm^{-1}, the further experiments are conducted by analyzing the region between 800 and 1700 cm^{-1} by using the objective magnification of 100x. Raman spectra are background subtracted and deconvolved by Lorentz line functions to derive peaks parameters such as position, amplitude and integrated intensity. In Figure 12, representative deconvolved Raman spectra of an aged paper sample containing lignin components and of a reference Whatman paper are shown.

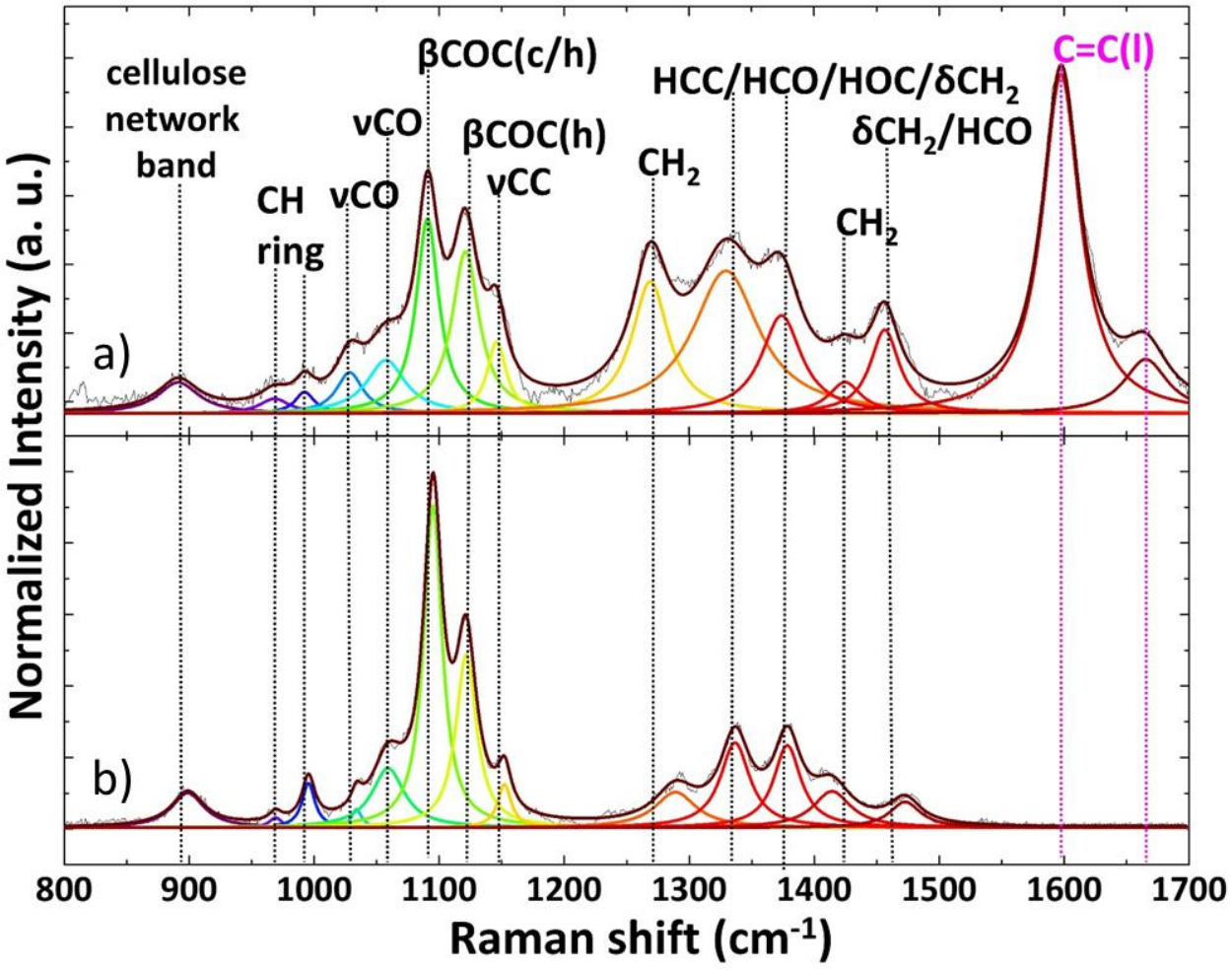

Figure 12 – Deconvolved Raman spectra of a) an aged paper sample containing lignin components and of b) Whatman paper.

As shown in Figure 12, both the spectra clearly show the signals ascribed to the cellulose phase. In addition, the Raman spectrum of the paper samples containing lignin (Fig. 12a) shows further peaks at around 1600 and 1650 cm^{-1} assigned to the C=C bonds in lignin units. In Table 1, the peak position and assignment for each signal are reported.

Table 1 – Peak position and assignment for the Raman signals.

Peak position (cm^{-1})	**Assignment**
900	Cellulose network band
960	CH ring vibrations
995	CH ring vibrations
1030	vCO bending modes
1052	vCO bending modes
1100	COC stretching of βglycosidic bonds in cellulose © chains
1120	COC stretching of βglycosidic bonds in cellulose © and hemicellulose (h) chains
1150	HCH asymmetric stretching
1340	CH (wagging), HCC, HOC, COH (rocking) bending
1380	CH (wagging), HCC, HOC, COH (rocking) bending
1430	HCH bending
1480	HOC bending and δCH2 scissors modes
1600	C=C
1640	C=C

The peaks parameters are valid tools to evaluate the conservation state and quality of papers:

(1) the cellulose network band at around 900 cm^{-1}, probably related with the lateral size of crystallites, is broad and less intensive as the size of cellulose crystallites are reduced in dimensions [32];

(2) the ratio between the βCOC and δCH2/HCO indicate different degrees of water accessibility within the cellulose matrix;

(3) the ratio between the lignin C=C peak at 1600 cm^{-1} and the βCOC allows to evaluate and compare the lignin content in different types of paper samples.

Raman spectral analysis, optimized as described, is a promising tool to characterize several paper samples features. In particular, the optimized procedure is useful to evaluate the effects produced by the irradiation tests on the structural features of both new and aged paper CH samples.

3.2 FTIR-ATR spectra

The FTIR spectra of the samples were acquired in transmission and ATR configuration. A typical FTIR spectrum of Whatman paper in transmission (ATR) in the range 400–4000 cm^{-1} is reported in Figure 13a (Fig. 13b).

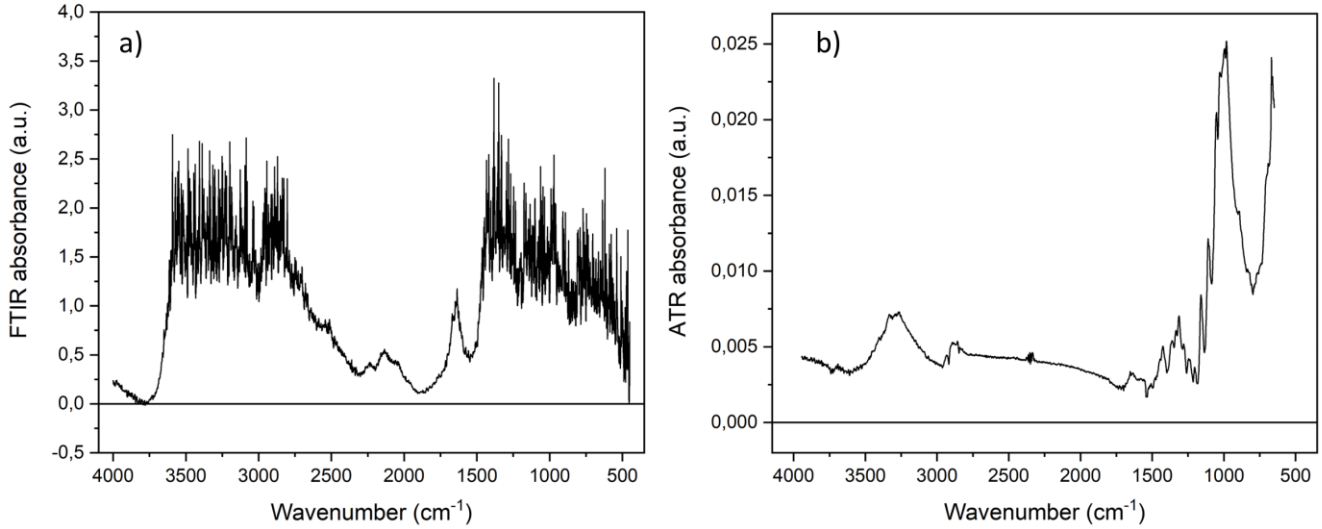

Figure 13 – FTIR spectrum of Whatman paper in the range 400 – 4000 cm^{-1} in a) transmission and b) ATR configuration.

To perform the analysis of each spectrum, the background (air) was subtracted and a correction of the baseline was done in the range 1830-1540 cm^{-1}. A fundamental parameter for the evaluation of paper oxidation state is the C=O peak area. For this reason, FTIR spectra were investigated in the range 1870-1525 cm^{-1} (Fig. 14) where the peaks corresponding to the bending mode of the adsorbed water molecules (1670 – 1630 cm^{-1}) and to the C=O stretching mode (1750 – 1710 cm^{-1}) are present [2], [33]–[35].

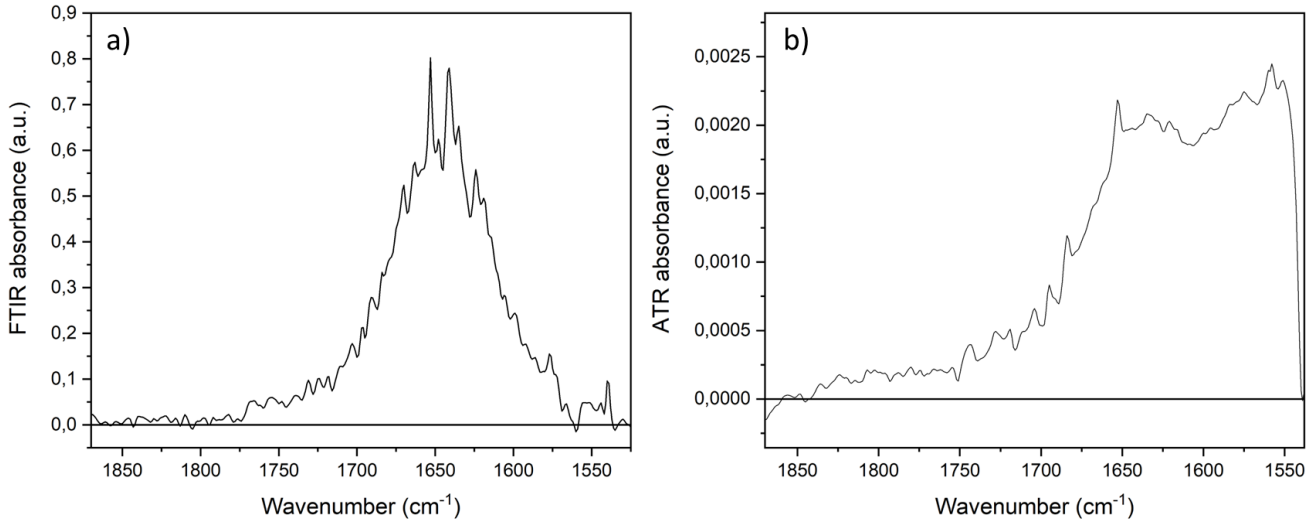

Figure 14 – FTIR spectra of Whatman paper in the range 1870-1525 cm^{-1} in a) transmission and b) ATR configuration.

From Figure 13 and Figure 14 it is evident that FTIR spectra acquired in transmission mode (Fig. 13a) are saturated in the regions below 1350 cm^{-1} and above 2800 cm^{-1} and thus the ATR spectra (Fig. 13b), for this kind of samples, are more useful for a general overview of the chemical bonds of the sample. Furthermore, ATR spectra allow the investigation of the OH band (3000-3600 cm^{-1}). Contrarily, in the range 1870-1525 cm^{-1}, the FTIR measurements in transmission (Fig. 14a) allows to evaluate the single contributions of the two bands corresponding to the C=O peak and to the adsorbed water peak hardly distinguishable in the ATR spectra (Fig. 14b). The FTIR spectra in transmission mode were thus chosen to check the oxidation state of paper samples.

To estimate the C=O peak area, that is partially overlapped with the peak corresponding to the adsorbed water, a multiple gaussian fit followed by a deconvolution was performed as reported for a Whatman paper sample in Figure 15.

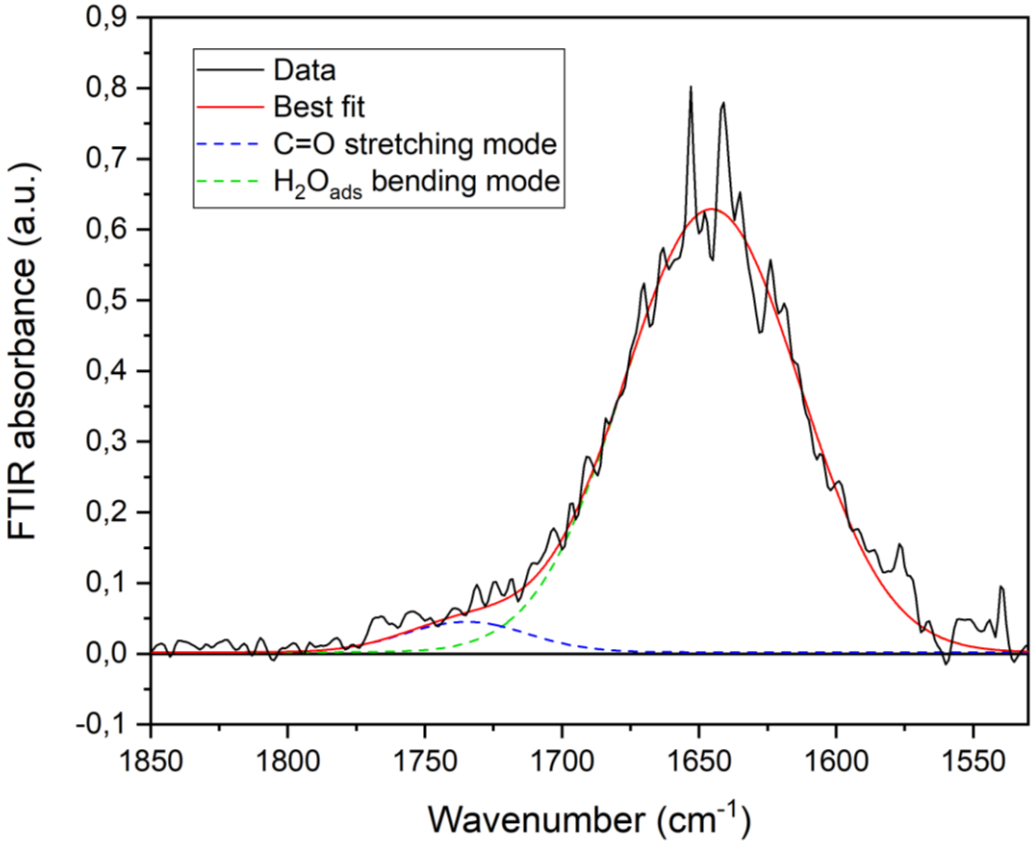

Figure 15 – FTIR spectrum of Whatman paper in the range 1850 – 1530 cm^{-1}. The black line represents the experimental data, the red line is the best double gaussian fit, the dashed blue line is the contribution of the C=O peak and the dashed green line is the one of the adsorbed water peak.

Three independent measurements were performed by removing and replacing the sample from the sample holder and the mean value of the analyzed parameter was used. The spread $\sigma_{C=O}$ of the C=O peak area value for the three performed measurements was calculated as:

$$\sigma_{C=O} = \frac{area_{max} - area_{min}}{2} \quad (2)$$

where $area_{max}$ and $area_{min}$ are the maximum and minimum C=O peak area value respectively of the set of measurements. The obtained value was about $\sigma_{C=O} = 3.8\%$.

By performing the above-described analysis on both the irradiated and not irradiated sample, it is possible to obtain the difference of the C=O peaks area values (C=O Δ-peak area) before and after irradiation. The C=O Δ-peak area was chosen to evaluate the paper oxidation due to the irradiation treatment. The C=O Δ-peak area error was calculated as:

$$\sigma_{\Delta-\text{peak area}} = \sqrt{\sigma_{C=O}^{before\ 2} + \sigma_{C=O}^{after\ 2}}$$

and it is $\sigma_{\Delta-\text{peak area}} = 5\%$.

The same procedure was performed to characterize the oxidation state of ancient paper. In addition, the reported protocol is successful to evaluate the variation of the oxidation degree of samples before and after gamma irradiation tests.

3.3 ESR spectra

To evaluate the quantity of free radicals created into the cellulose network after irradiation and to study their behavior, ESR measurements were performed in the range 3400 – 3550 G. Both Whatman and ancient paper do not show an ESR signal before irradiation (no radicals present). Gamma radiation exposure induces the formation of many kind of free radicals on the cellulose network: some of them are characterized by a very long life time (years) while others are unstable and may react with the surrounding molecules in a short time. Therefore, it is crucial to perform the paper ESR measurements right after the irradiation.

The ESR spectrum of paper after irradiation is the result of a superimposition of hardly distinguishable and separable contributions (singlet, doublet, triplet), corresponding to different radicalic species on the cellulose structure [36], [37], as shown for Whatman paper in Figure 16.

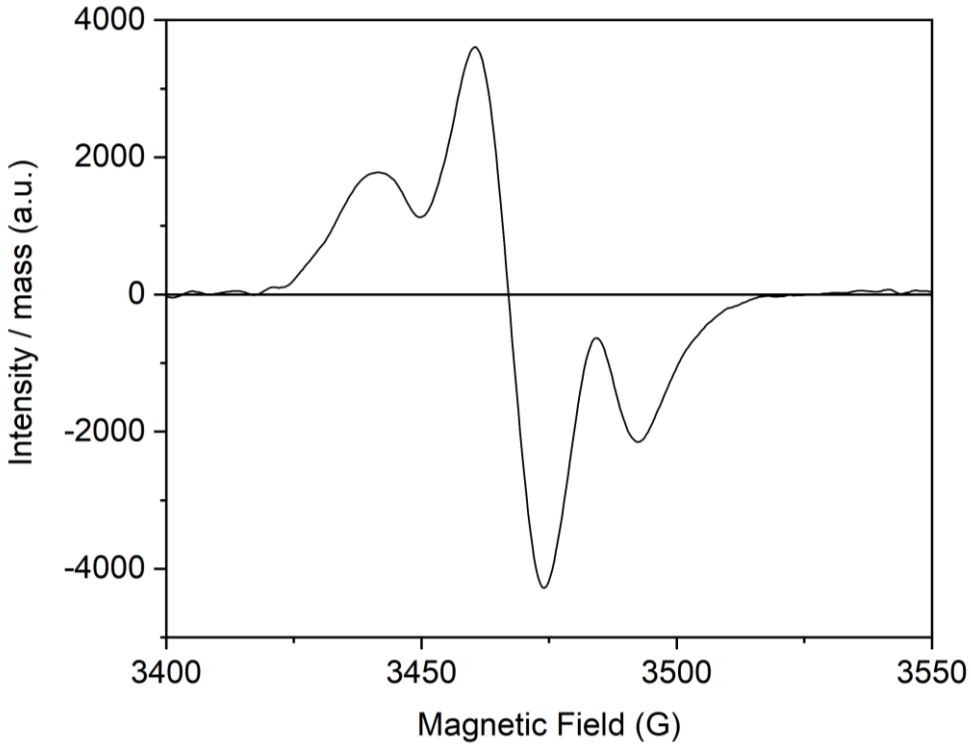

Figure 16 – ESR spectrum of Whatman paper after irradiation.

Therefore, in this study, the maximum peak-to-peak height (often considered in the ESR analysis and proportional to the free radicals number) cannot be used as single reliable indicator of the radicals amount and the whole ESR spectrum is always processed and analyzed. In particular, by integrating the ESR spectrum, the absorbance spectra were obtained for each irradiated Whatman sample, as shown as an example in Figure 17.

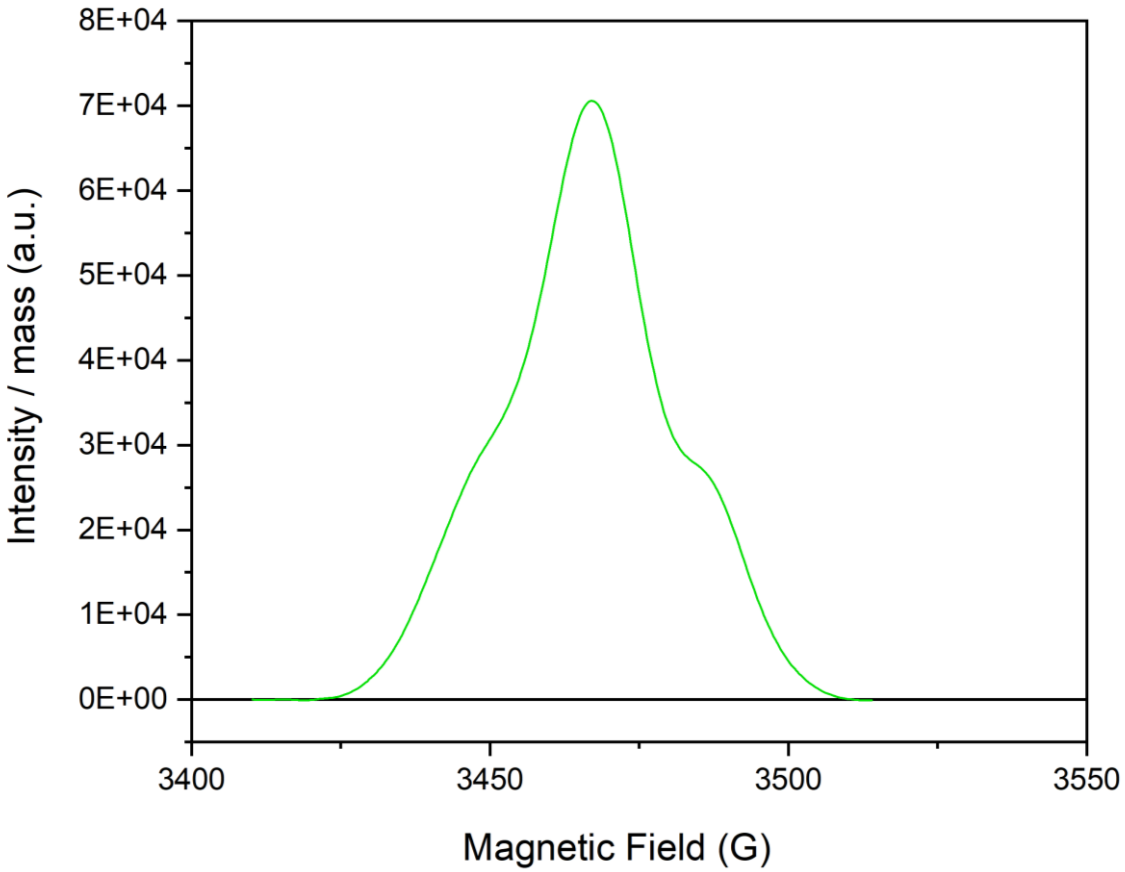

Figure 17 – Integral of the ESR spectrum of a Whatman sample after irradiation.

The area of the physical signal (absorbance spectrum) was then obtained and used as parameter for the paper characterization. This value is proportional to the number of radicals present in the samples and to the samples mass. Therefore, to compare signals from different samples, all the ESR spectra were normalized to the sample mass before the data analysis. In this ESR investigation, samples consist in strips of paper positioned into a vertical quartz tube and then inserted into the microwave cavity. Quartz tubes are employed in ESR spectroscopy because they do not have a signal. In particular, a quartz tube of 6 mm diameter was used for this study. It is important that a paper strip is not larger than the cavity, otherwise the induced radicals in part of the sample will be not effectively detected by the instrument although the considered sample mass is that of the full strip. An optimization of the measurement procedure was thus set up for the cavity of the ESR spectrometer used in this study. An irradiated alanine pellet (a dosimeter with a stable ESR signal and a thickness

of about 2 mm) was positioned in a conventional quartz tube, many measurements were acquired by placing the tube and thus the pellet at different heights *z* with respect to the top of the spectrometer's case. For each position of the tube, a spectrum of the alanine pellet was acquired and analyzed, so characterizing the sensitivity of different portions of the cavity. By plotting the area of the detected signals as a function of *z* (Fig. 18), the height at which the signal is maximized was found and the length of the sample strip to be used was chosen as the full width at half maximum of the obtained profile.

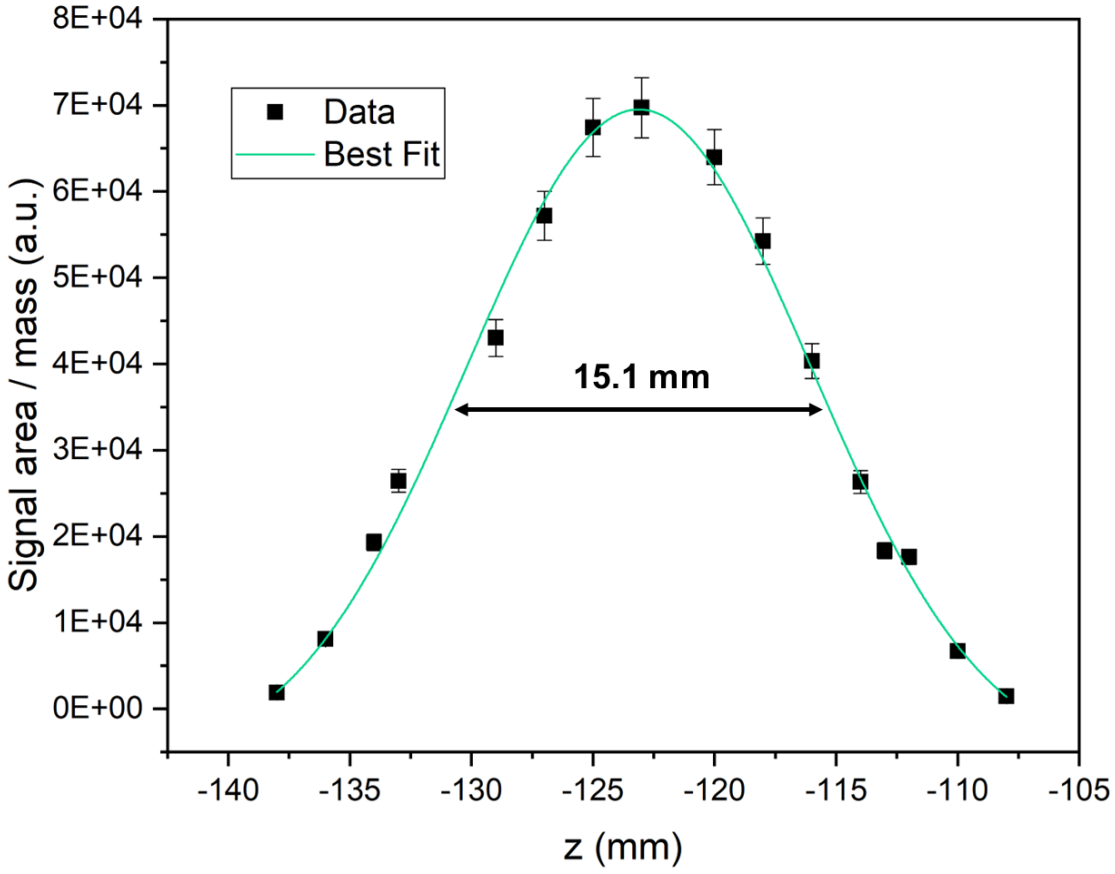

Figure 18 – Alanine pellet ESR signal area as a function of the height *z*.

As a result of the optimization procedure, a sample strip of about 15 mm is recommended. An example of the difference of the ESR spectra normalized to the sample mass, obtained with two strips of the same sample but of different lengths, is reported in Fig. 19.

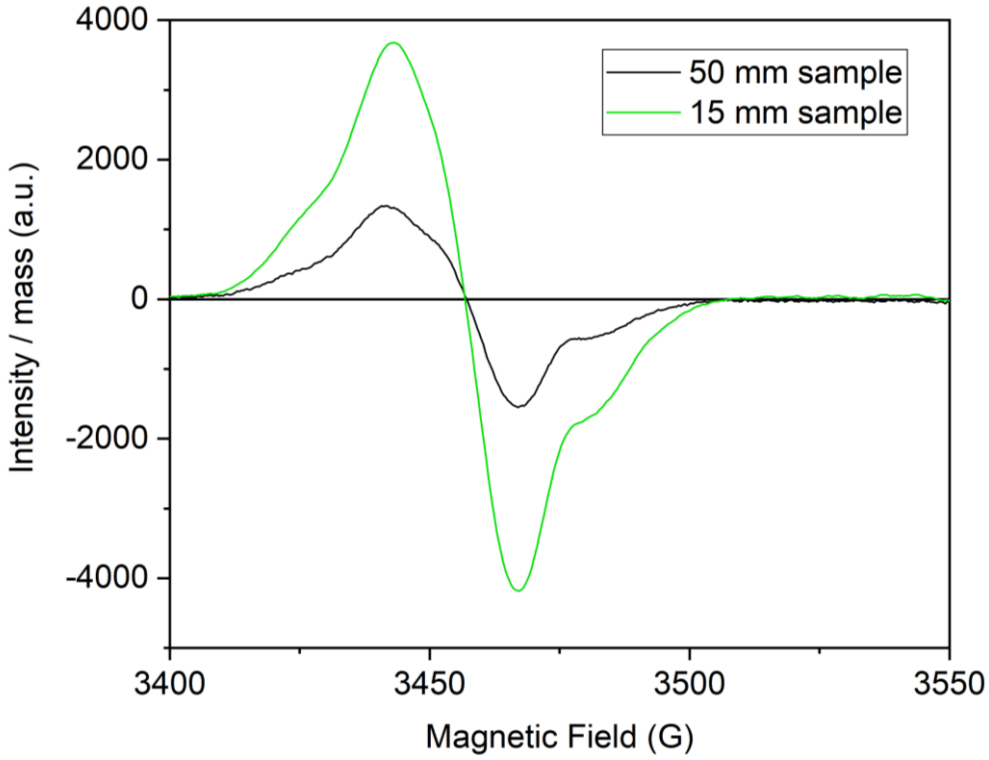

Figure 19 – ESR spectra of Whatman paper after irradiation, acquired for two strips of the same sample having different length.

The error associated with the calculation of the signal area was calculated as the spread of the signal area value on three repeated measurements. It is about $\sigma_{\mathrm{ESR\ area}} = 5\%$.

3.4 Viscosimetric analysis

To evaluate the viscosity variation of the paper before and after irradiation, the procedure described in the ISO:5351:2012 standard regulation was followed [14]. Three independent measurements of 850 µl of cupriethylenediamine (CED) were performed before samples measurements. Then, for each sample, 12 mg of paper were dissolved in 3.4 ml of CED 0.5 M by mixing for three minutes the solution of paper sample and CED in a plastic cuvette. Three different viscosity measurements (850 µl of solution each) were performed and the average value was used for the calculations. Through the value of the viscosity of the solvent $\eta_{solvent}$ and the viscosity of the cellulose containing solution ($\eta_{solution}$), it was possible to obtain the relative viscosity η_{rel} with the formula:

$$\eta_{rel} = \frac{\eta_{solution}}{\eta_{solvent}} \ . \qquad (3)$$

The choice of 12 mg as sample weight is linked to the table of ISO:5351:2012 standard regulation Annex B [14] that reports the values of $[\eta_{intr}] \cdot \rho$ (where ρ is the concentration of cellulose in CED solution and η_{intr} is the intrinsic viscosity) corresponding to different η_{rel}. In

detail, after numerous attempts with many sample mass values, it was found that 12 mg was in agreement with the values of η_{rel} ($\eta_{rel} > 1$) reported in the table of the Annex B.

The η_{intr} value was thus calculated by dividing the obtained product $[\eta_{intr}] \cdot \rho$ for the concentration ρ. Afterwards, the DP was calculated by the Mark-Houwink-Sakurada equation:

$$DP^{\alpha} = k \cdot \eta_{intr} \tag{4}$$

where k and α are constants related to the solvent and the polymer type (for cellulose: k = 0.75 and α = 0.905) [38], [39].

The measurements uncertainty was obtained by the spread σ_{visc} of three values of DP calculated for the not irradiated sample and it was about $\sigma_{visc} = 3\%$.

3.5 Colorimetric analysis

The samples color was shown in the CIE 1931 xyY (reported in Figure 20 as example for not irradiated Whatman paper) and in the CIELAB color space.

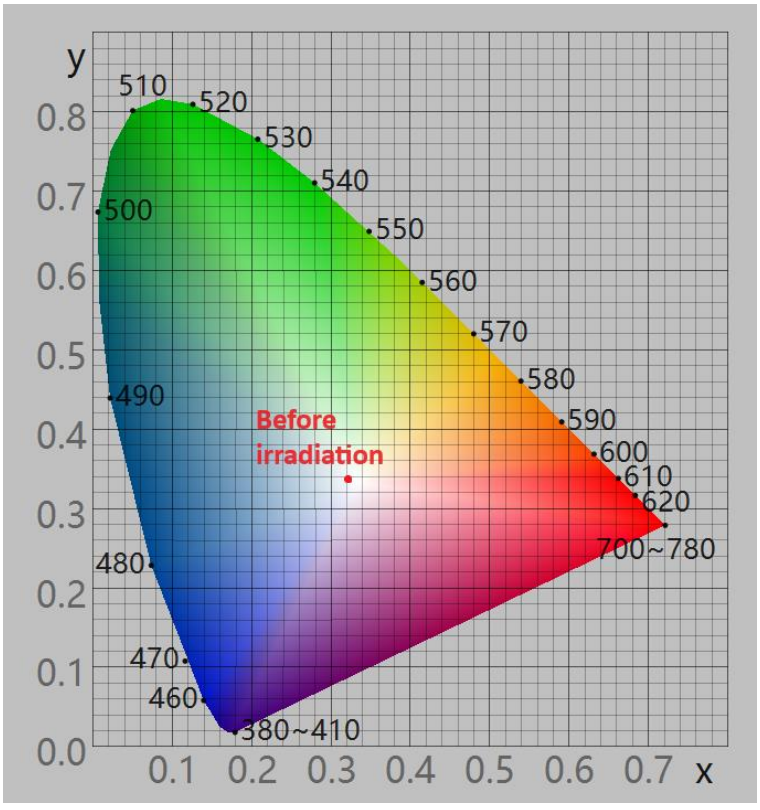

Figure 20 – Whatman paper color before irradiation represented in the CIE 1931 xyY color space.

To obtain the color coordinates and the relative error, one measurement was performed at the center of the sample and ten independent measurements were performed on different

points of the sample. The spread σ_{col}^{ref} of the Δ*E**, corresponding to the color difference between the center and other points of the sample of the reference paper, was about $\sigma_{col}^{ref} = 1\%$. Conversely, ancient papers are characterized by a high inhomogeneity of color (e.g. for molds and fungi presence). Therefore, by measuring one point at the center of the sample (marked as Reference in Fig. 21) and by repeating the colorimetric measurements on different points (highlighted in Fig. 21) the spread associated with the Δ*E** value was about $\sigma_{col}^{ancient}$ = 30%.

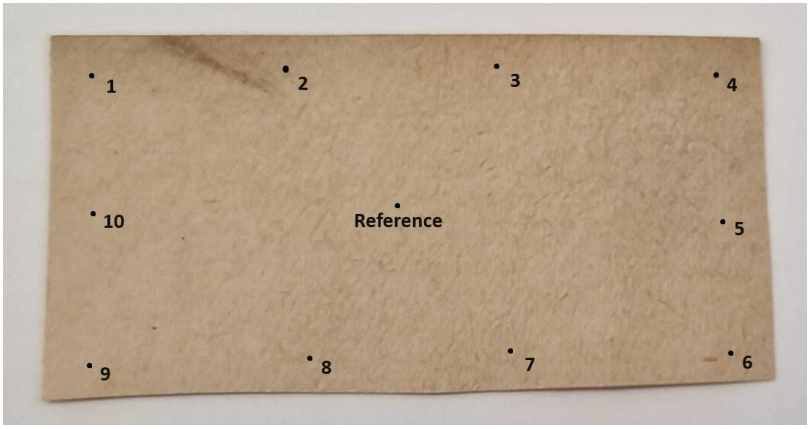

Figure 21 – Ancient paper sample with colorimetric measurements points.

Therefore, the measurement before and after irradiation on ancient paper samples are always performed on the same point of the sample. In this way, only the color variation possibly caused by gamma radiation and not by the sample color inhomogeneity is measured.

4 Conclusion

This report is focused on optimizing the characterization procedures of paper samples to allow an evaluation of the effects induced by gamma radiation on Cultural Heritage artworks. The techniques described are useful to characterize many microscopic and macroscopic features of papery samples, enabling a comparison of the sample's characteristics before and after irradiation. Furthermore, the choice of these experimental techniques for the characterization of the samples has tried to privilege the availability and ease-to-use of methods not invasive and not destructive as much as possible, providing a valid and reproducible procedure.

Acknowledgements

We thank the staff of the Laboratory of Solar Technology Engineering (TERIN-STSN-ITES) of ENEA Casaccia R.C. that made the rheometer available to us to do the above-reported viscosimetric analysis and Alessia Embriaco of the National Institute of Ionizing Radiation Metrology (FSN-IMRI) for the help with the ESR cavity characterization.

References

[1] M. Adamo, S. Baccaro, and A. Cemmi, “Radiation processing for bio-deteriorated archived materials and consolidation of porous artefacts,” *ENEA Tech. Rep. RT/2015/5/ENEA*, 2015.

[2] S. Baccaro, M. Carewska, C. Casieri, A. Cemmi, and A. Lepore, “Structure modifications and interaction with moisture in γ-irradiated pure cellulose by thermal analysis and infrared spectroscopy,” *Polym. Degrad. Stab.*, vol. 98, no. 10, pp. 2005–2010, Oct. 2013, doi: 10.1016/J.POLYMDEGRADSTAB.2013.07.011.

[3] K. T. Gillen, R. L. Clough, and N. J. Dhooge, “Density profiling of polymers,” *Polymer (Guildf).*, vol. 27, no. 2, pp. 225–232, Feb. 1986, doi: 10.1016/0032-3861(86)90330-7.

[4] I. V. Moise *et al.*, “Establishing the irradiation dose for paper decontamination,” *Radiat. Phys. Chem.*, vol. 81, no. 8, pp. 1045–1050, Aug. 2012, doi: 10.1016/J.RADPHYSCHEM.2011.11.063.

[5] I. V. Moise *et al.*, “The crosslinking behaviour of cellulose in gamma irradiated paper,” *Polym. Degrad. Stab.*, vol. 160, pp. 53–59, Feb. 2019, doi: 10.1016/J.POLYMDEGRADSTAB.2018.12.005.

[6] M. C. Area, A. M. Calvo, F. E. Felissia, A. Docters, and M. V. Miranda, “Influence of dose and dose rate on the physical properties of commercial papers commonly used in libraries and archives,” *Radiat. Phys. Chem.*, vol. 96, pp. 217–222, Mar. 2014, doi: 10.1016/J.RADPHYSCHEM.2013.10.004.

[7] M. Bicchieri, M. Monti, G. Piantanida, and A. Sodo, “Effects of gamma irradiation on deteriorated paper,” *Radiat. Phys. Chem.*, vol. 125, pp. 21–26, Aug. 2016, doi: 10.1016/J.RADPHYSCHEM.2016.03.005.

[8] O. H. A. Fernández and I. Fofana, “Aging Characterization of Electrical Insulation Papers Impregnated with Synthetic Ester and Mineral Oil : Correlations Between Mechanical Properties , Depolymerization and Some Chemical Markers,” *IEEE Trans. Dielectr. Electr. Insul.*, vol. 25 no.1, no. November 2017, pp. 217–227, 2017, doi: 10.1109/TDEI.2018.006317.

[9] Cytiva, “Whatman.” [Online]. Available: https://www.cytivalifesciences.com/en/us/about-us/our-brands/whatman

[10] A. Lepore, S. Baccaro, C. Casieri, A. Cemmi, and F. De Luca, “Role of water in the ageing mechanism of paper,” *Chem. Phys. Lett.*, vol. 531, pp. 206–209, Apr. 2012, doi: 10.1016/J.CPLETT.2012.01.083.

[11] S. Baccaro, A. Cemmi, I. Di Sarcina, and G. Ferrara, “Gamma Irradiation CALLIOPE Facility at ENEA Casaccia Research Centre,” *ENEA Tech. Rep. RT/2015/13/ENEA*, 2015.

[12] Bruker, “Guide to Infrared Spectroscopy.” [Online]. Available: https://www.bruker.com/it/products-and-solutions/infrared-and-raman/ft-ir-routine-spectrometer/what-is-ft-ir-spectroscopy.html

[13] L.- Chemistry, “EPR - Theory.” [Online]. Available: https://chem.libretexts.org/Bookshelves/Physical_and_Theoretical_Chemistry_Textbook_Maps/Supplemental_Modules_(Physical_and_Theoretical_Chemistry)/Spectroscopy/Magnetic_Resonance_Spectroscopies/Electron_Paramagnetic_Resonance/EPR_-_Theory

[14] ISO/5351, “ISO 5351:2010, Determination of limiting viscosity number in cupri-ethylenediamine (CED) solution.” Accessed: Dec. 01, 2023. [Online]. Available: https://www.iso.org/obp/ui/#iso:std:iso:5351:ed-2:v1:en

[15] A. Paar, “Viscosity and Viscosimetry.” [Online]. Available: https://wiki.anton-paar.com/en/basic-of-viscometry/#:~:text=The shear rate is the,second %5Bs-1%5D.&text=According to Newton’s Law%2C shear,stress divided by shear rate.

[16] J. Schanda, “Colorimetry: Understanding the CIE System,” *Color. Underst. CIE Syst.*, pp. 1–459, Mar. 2007, doi: 10.1002/9780470175637.

[17] ISO/5631-2, “ISO 5631-2:2015 - Paper and board — Determination of colour by

diffuse reflectance — Part 2: Outdoor daylight conditions (D65/10 degrees)." Accessed: Dec. 04, 2023. [Online]. Available: https://www.iso.org/standard/67155.html

[18] F. Coppola, F. Fiorillo, A. Modelli, M. Montanari, and M. Vandini, "Effects of γ-ray treatment on paper," *Polym. Degrad. Stab.*, vol. 150, pp. 25–30, Apr. 2018, doi: 10.1016/J.POLYMDEGRADSTAB.2018.02.004.

[19] G. Hoffmann, "CIELab Color Space." [Online]. Available: http://docs-hoffmann.de/cielab03022003.pdf

[20] W. Mokrzycki Cardinal Stefan and M. Tatol, "Color difference Delta E-A survey Colour difference ΔE-A survey," *Mach. Graph. Vis*, vol. 20, no. 4, pp. 383–411, 2011.

[21] A. P. P. Alves *et al.*, "The structure of different cellulosic fibres characterized by Raman spectroscopy," *Vib. Spectrosc.*, vol. 86, pp. 324–330, Sep. 2016, doi: 10.1016/J.VIBSPEC.2016.08.007.

[22] C. Yan *et al.*, "Analysis of handmade paper by Raman spectroscopy combined with machine learning," *J. Raman Spectrosc.*, vol. 53, no. 2, pp. 260–271, Feb. 2022, doi: 10.1002/JRS.6280.

[23] J. Zięba-Palus, A. Wesełucha-Birczyńska, B. Trzcińska, R. Kowalski, and P. Moskal, "Analysis of degraded papers by infrared and Raman spectroscopy for forensic purposes," *J. Mol. Struct.*, vol. 1140, pp. 154–162, Jul. 2017, doi: 10.1016/J.MOLSTRUC.2016.12.012.

[24] D. Chiriu, P. C. Ricci, G. Cappellini, M. Salis, G. Loddo, and C. M. Carbonaro, "Ageing of ancient paper: A kinetic model of cellulose degradation from Raman spectra," *J. Raman Spectrosc.*, vol. 49, no. 11, pp. 1802–1811, Nov. 2018, doi: 10.1002/JRS.5462.

[25] S. Botti, F. Bonfigli, V. Nigro, A. Rufoloni, and A. Vannozzi, "Evaluating the Conservation State of Naturally Aged Paper with Raman and Luminescence Spectral Mapping: Toward a Non-Destructive Diagnostic Protocol," *Mol. 2022, Vol. 27, Page 1712*, vol. 27, no. 5, p. 1712, Mar. 2022, doi: 10.3390/MOLECULES27051712.

[26] M. Bicchieri, F. Valentini, A. Calcaterra, and M. Talamo, "Newly Developed Nano-

Calcium Carbonate and Nano-Calcium Propanoate for the Deacidification of Library and Archival Materials," *J. Anal. Methods Chem.*, vol. 2017, 2017, doi: 10.1155/2017/2372789.

[27] D. Chiriu, P. C. Ricci, G. Cappellini, and C. M. Carbonaro, "Ancient and modern paper: Study on ageing and degradation process by means of portable NIR μ-Raman spectroscopy," *Microchem. J.*, vol. 138, pp. 26–34, May 2018, doi: 10.1016/J.MICROC.2017.12.024.

[28] U. P. Agarwal, "Beyond Crystallinity: Using Raman Spectroscopic Methods to Further Define Aggregated/Supramolecular Structure of Cellulose," *Front. Energy Res.*, vol. 10, p. 857621, Apr. 2022, doi: 10.3389/FENRG.2022.857621/BIBTEX.

[29] A. L. P. Queiroz *et al.*, "Investigating microcrystalline cellulose crystallinity using Raman spectroscopy," *Cellulose*, vol. 28, no. 14, pp. 8971–8985, Sep. 2021, doi: 10.1007/S10570-021-04093-1/FIGURES/8.

[30] U. P. Agarwal, "Detection and quantitation of cellulose II by Raman spectroscopy," 2021, doi: 10.21203/rs.3.rs-661415/v1.

[31] V. V. Nosenko, A. M. Yaremko, V. M. Dzhagan, I. P. Vorona, Y. A. Romanyuk, and I. V. Zatovsky, "Nature of some features in Raman spectra of hydroxyapatite-containing materials," *J. Raman Spectrosc.*, vol. 47, no. 6, pp. 726–730, Jun. 2016, doi: 10.1002/JRS.4883.

[32] M. Szymańska-Chargot, J. Cybulska, and A. Zdunek, "Sensing the Structural Differences in Cellulose from Apple and Bacterial Cell Wall Materials by Raman and FT-IR Spectroscopy," *Sensors 2011, Vol. 11, Pages 5543-5560*, vol. 11, no. 6, pp. 5543–5560, May 2011, doi: 10.3390/S110605543.

[33] D. Ciolacu, F. Ciolacu, and V. I. Popa, "AMORPHOUS CELLULOSE-STRUCTURE AND CHARACTERIZATION," *Cellul. Chem. Technol. Cellul. Chem. Technol*, vol. 45, no. 2, pp. 13–21, 2011.

[34] J. Łojewska, A. Lubańska, P. Miśkowiec, T. Łojewski, and L. M. Proniewicz, "FTIR in situ transmission studies on the kinetics of paper degradation via hydrolytic and oxidative reaction paths," *Appl. Phys. A Mater. Sci. Process.*, vol. 83, no. 4, pp. 597–603, Jun. 2006, doi: 10.1007/S00339-006-3529-9/METRICS.

[35] A. Cemmi, I. Di Sarcina, and B. D'Orsi, "Gamma radiation-induced effects on paper irradiated at absorbed doses common for cultural heritage preservation," *Radiat. Phys. Chem.*, vol. 202, p. 110452, Jan. 2023, doi: 10.1016/J.RADPHYSCHEM.2022.110452.

[36] H. Kameya and M. Ukai, "Analysis of Relaxation Behavior of Free Radicals in Irradiated Cellulose Using Pulse and Continuous-Wave Electron Spin Resonance," *Cellul. - Fundam. Asp.*, Aug. 2013, doi: 10.5772/51634.

[37] Y. Kodama, O. Rodrigues, R. H. L. Garcia, P. de S. Santos, and P. A. S. Vasquez, "Study of free radicals in gamma irradiated cellulose of cultural heritage materials using Electron Paramagnetic Resonance," *Radiat. Phys. Chem.*, vol. 124, pp. 169–173, Jul. 2016, doi: 10.1016/J.RADPHYSCHEM.2016.02.018.

[38] P.J. Flory, *Principles of Polymer Chemistry*. Cornell University Press, New York, 1953.

[39] C. Tanford, *Physical Chemistry of Macromolecules*. 1962.

ENEA
Servizio Promozione e Comunicazione
www.enea.it

Stampa: Laboratorio Tecnografico ENEA - C.R. Frascati
febbraio 2024